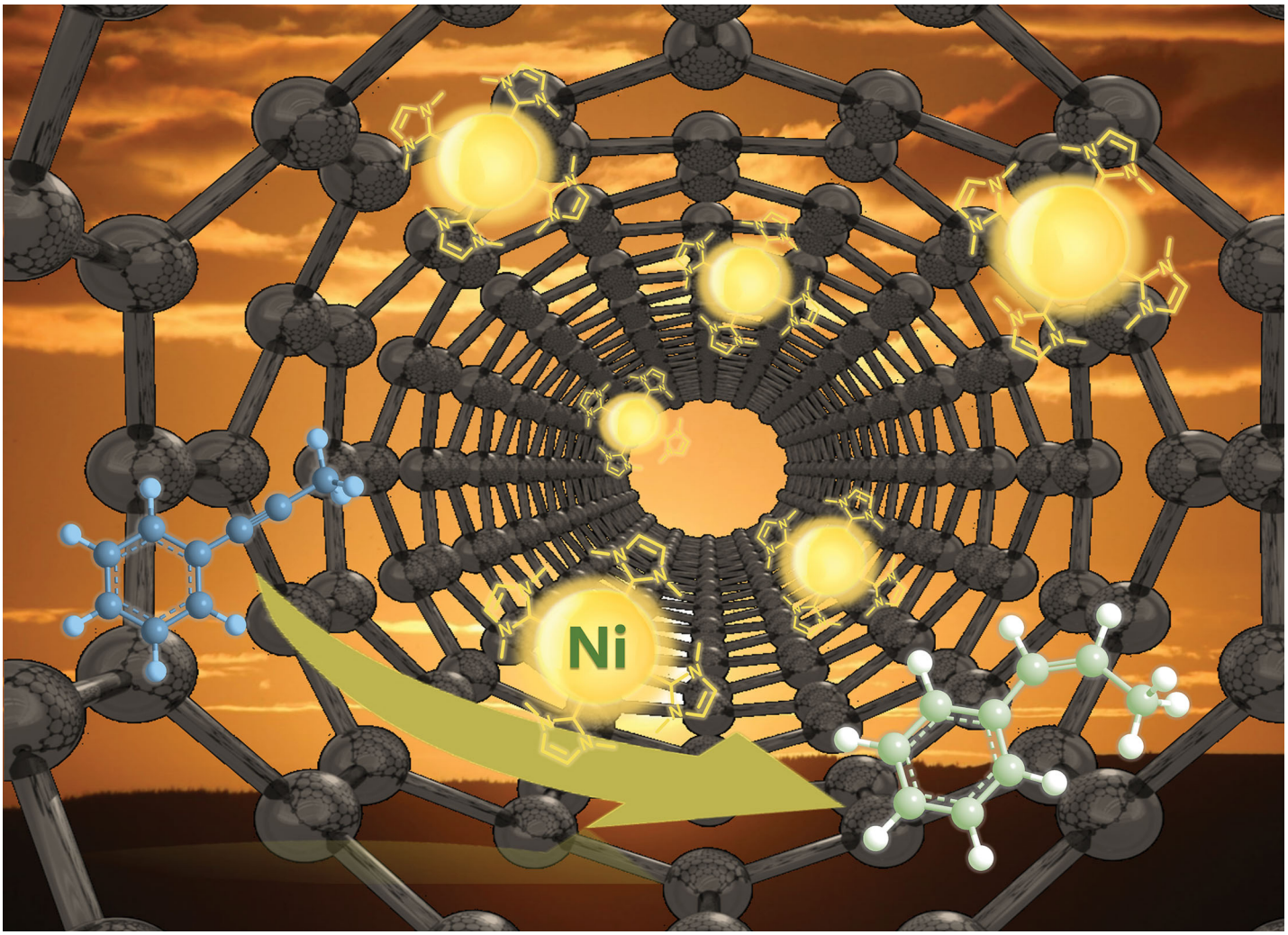

Showcasing research from Department of Catalysis, Chemistry Technology Center, Tarragona, Spain.

Facile synthesis of NHC-stabilized Ni nanoparticles and their catalytic application in the *Z*-selective hydrogenation of alkynes

Make it easy selecting the right NHC precursor! In their communication on page 7894, Miriam Díaz de los Bernardos, Carmen Claver, Cyril Godard and co-workers describe a new and straightforward methodology for the preparation small and well defined NHC-stabilized nickel nanoparticles *via* the decarboxylation of 1,3-dialkylimidazolium-2-carboxylate. These nanoparticles provided excellent activities and selectivities in the partial hydrogenation of alkynes into (*Z*)-alkenes under very mild reaction conditions.

As featured in:

See Miriam Díaz de los Bernardos, Cyril Godard *et al.*, *Chem. Commun.*, 2017, **53**, 7894.

ROYAL SOCIETY OF CHEMISTRY

rsc.li/chemcomm

Registered charity number: 207890

ChemComm

COMMUNICATION

View Article Online
View Journal | View Issue

Check for updates

Cite this: *Chem. Commun.*, 2017, 53, 7894

Received 8th March 2017,
Accepted 27th April 2017

DOI: 10.1039/c7cc01779k

rsc.li/chemcomm

Facile synthesis of NHC-stabilized Ni nanoparticles and their catalytic application in the *Z*-selective hydrogenation of alkynes†

Miriam Díaz de los Bernardos,‡*[a] Sara Pérez-Rodríguez,‡[a] Aitor Gual,[a] Carmen Claver[ab] and Cyril Godard[ab]*

Well defined Ni nanoparticles (NiNPs) stabilized with N-heterocyclic carbenes (NHCs) have been synthesized through a new methodology involving the decarboxylation of a zwitterionic CO_2 adduct. Their catalytic performance was tested in the partial hydrogenation of alkynes into (*Z*)-alkenes under very mild reaction conditions (50 °C and 5 bar H_2 pressure), providing excellent activities and selectivities.

Metal nanoparticles (MNPs) display unique physical and chemical properties, which endow them with high potential for applications in diverse areas such as medicine and catalysis, among others.[1,2] To enhance their performance in catalysis, the selective formation of well-defined nano-objects is required. Furthermore, they should be stabilized with species that will restrict the approach of the substrate and as such induce selectivity. Nowadays, N-heterocyclic carbenes (NHCs) constitute one of the most versatile family of compounds in modern chemistry and are employed as ligands in transition metal catalysed transformations in both academia and the chemical industry.[3] Although these ligands were used for the preparation of Au,[4–8] Pd,[9] Ir[10] and Ru[11,12] nanoparticles, to the best of our knowledge, there is only one report on the use of NHCs for the stabilization of Ni NPs.[13] To date, NHC-stabilized MNPs have been obtained by three main methodologies: (i) by direct reduction of NHC–organometallic complexes,[6] (ii) by procedures using the isolated free carbene (either by ligand exchange[14] or by the organometallic approach developed by Chaudret[11]), and (iii) using non-isolable carbenes *via in situ* generation of free carbenes (Scheme 1).[12]

In all cases, a basic pre-treatment of an imidazolium salt precursor is required, either for the isolation of the free carbene or for its *in situ* generation. Crabtree *et al.* reported the utilization of 1,3-dialkylimidazolium-2-carboxylate (**R_2Im-CO_2**) as an efficient carbene precursor for the synthesis of NHC-based organometallic complexes.[15]

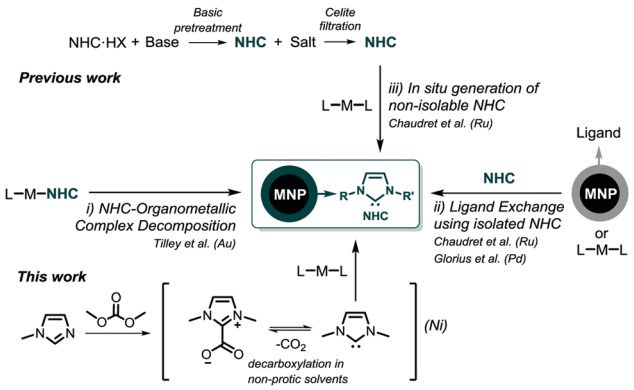

Scheme 1 Synthetic approaches to NHC-stabilized metal nanoparticles.

These imidazolium carboxylates are water-stable and synthetically readily available, and efficiently transfer the corresponding NHC ligand by decarboxylation in non-polar solvents.[16,17] It was therefore thought that the use of such NHC-precursors could be applied in the synthesis of MNPs, and as such, neither the filtration of inorganic salts nor the isolation of carbenes would be required.

The hydrogenation of alkynes to selectively produce (*E*)- or (*Z*)-alkenes is a useful synthetic tool for the production of valuable compounds.[18] Since classical heterogeneous catalysts are usually based on noble metals such as Pd, Pt or Au,[19–22] new approaches employing abundant and low-cost metals are therefore desirable. Recently, Prechtl and co-workers reported the use of NiNPs stabilised with ionic liquids for the selective hydrogenation of alkynes to the corresponding (*Z*)-alkenes.[20]

Here, we report a new and straightforward methodology to prepare small and well defined NHC-stabilized nickel nanoparticles, both colloidal and supported on carbon nanotubes (CNTs), using a simple "one-pot" procedure based on the decarboxylation of 1,3-dialkylimidazolium-2-carboxylate (**R_2Im-CO_2**).[23] This procedure avoids basic pre-treatment. The catalytic performance

[a] *Centre Tecnològic de la Química, Marcel·lí Domingo s/n, Campus Sescelades, 43007 Tarragona, Spain*
[b] *Departament de Química Física i Inorgánica, Universitat Rovira i Virgili, Marcel·lí Domingo s/n, Campus Sescelades, 43007 Tarragona, Spain. E-mail: Cyril.godard@urv.cat*

† Electronic supplementary information (ESI) available. See DOI: 10.1039/c7cc01779k
‡ These authors contributed equally to the experimental work.

of the latter species was evaluated in the selective hydrogenation of internal alkynes into *Z*-alkenes under mild conditions.

To evaluate **Me_2Im-CO_2** as a ligand precursor for the stabilization of NiNPs, the organometallic precursor $Ni(COD)_2$ (COD = cyclooctadiene) was reduced in THF under 3 bar of hydrogen at 60 °C in the presence of **Me_2Im-CO_2** (Scheme 2). The amount of the NHC-based ligand used during the synthesis was varied: 0.1, 0.2, 0.5 and 1 equivalent per Ni.

In the presence of 0.1 equivalent of the ligand, nickel particles were not efficiently stabilized. When the amount of the ligand was increased, the NPs **Ni-0.2**, **Ni-0.5** and **Ni-1** were formed and could be isolated. The TEM images of these particles are shown in Fig. 1.

As previously observed with NHCs,[11] smaller NPs were formed upon increasing the amount of the ligand from 0.2 to 0.5 equivalent per Ni. Indeed, in the **Ni-0.2** sample, the NPs exhibited a mean diameter of *ca.* 2.4 ± 0.9 nm, whilst for **Ni-0.5**, the mean size was *ca.* 2.0 ± 0.4 nm. Under these conditions, the particles were well separated and neither agglomeration nor coalescence was detected on the carbon grid, indicating that the NHC-based ligand is strongly adsorbed on the nickel surface. However, for **Ni-1** NPs a mean diameter of *ca.* 2.9 ± 0.7 nm was measured and a high degree of agglomeration was observed.

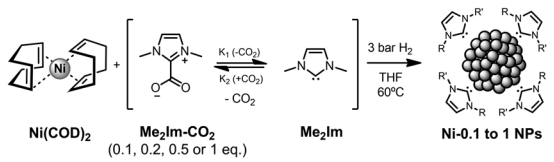

Scheme 2 Synthetic methodology used for the preparation of NHC-stabilized NiNPs using **Me_2Im-CO_2** as a stabilizer precursor.

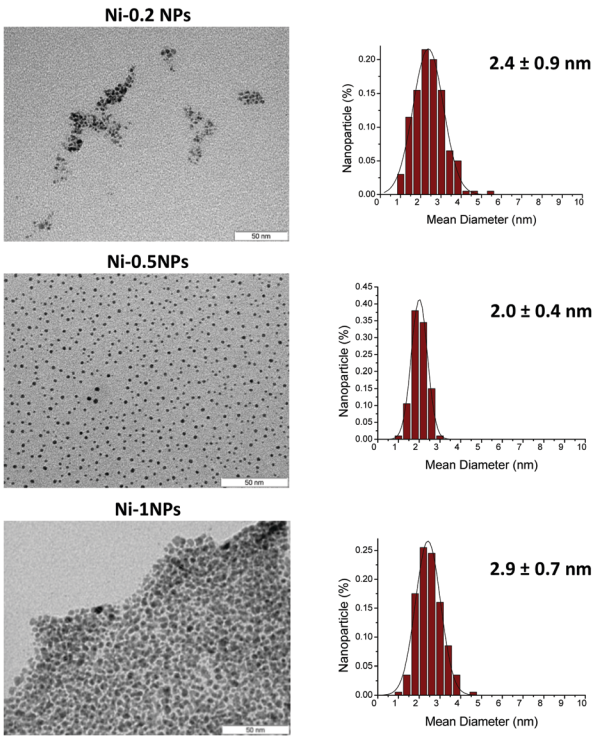

Fig. 1 TEM micrographs and size distributions of **Ni-0.2**, **Ni-0.5** and **Ni-1** nanoparticles.

TGA of the samples revealed that the NHC content for these NPs ranges from *ca.* 15 wt% (**Ni-0.2** NPs) to 44 wt% (**Ni-1.0** NPs) (Fig. S1, ESI†). **Ni-0.5** NPs presented a ligand content of 27 wt%. Similar NHC contents were previously reported for Ru[24] and Pt[25] NPs. In addition, no weight loss associated with the presence of imidazolium carboxylate (at *ca.* 200 °C) was observed, confirming that this species does not act as a stabilizer. XRD patterns of a selected sample (**Ni-0.5** NPs, Fig. S3, ESI†) revealed the presence of crystalline Ni with fcc packing. XPS measurements (Fig. S4, ESI†) showed a high percentage of NiO on the surface of the Ni nanoparticles (67.6 at%), which was attributed to nanoparticle oxidation during the sample preparation for XPS analysis. Indeed, nickel nanoparticles are very reactive and burn spontaneously in the presence of air, producing white clouds of the oxide, which is explained by their very small size and clean surface state. Upon Ar sputtering, the Ni content substantially increased (from 32.4 to 95.5 at%), confirming the presence of metal core nanoparticles. This new route was first validated by comparing two batches of NiNPs stabilized with 1,3-dimethylimidazol-2-ylidene (**Me_2Im**), prepared by (i) the abovementioned methodology and (ii) the reported *in situ* generation of non-isolable NHCs,[12] which is first employed here for the preparation of Ni nanoparticles. Following the last protocol, Me_2Im·HCl (0.5 molar equiv./Ni) was deprotonated *via* the addition of a slight excess of KOtBu in THF, and the resulting suspension (**Me_2Im**) was filtered through celite prior to its transfer into a solution of $Ni(COD)_2$ in THF. The reaction mixture was then pressurized with 3 bar of H_2, leading to a colloidal solution of nickel NPs with a mean size of 2.0 ± 0.5 nm (Fig. S5, ESI†). Comparison with the TEM data obtained by the new methodology clearly revealed similar dispersion of the particles on the grid and size (2.0 ± 0.4 nm). In addition, the IR spectra recorded for the two batches of **Ni-Me_2Im** NPs were similar. In the sample of NPs prepared *via* the decarboxylation method, the characteristic features of the **Me_2Im-CO_2** compound were not detected, confirming that this species does not participate in the NP stabilization (Fig. S6, ESI†). Furthermore, the TGA data recorded for the two batches of **Ni/Me_2Im** NPs showed similar profiles (Fig. S7, ESI†). Based on these results, it was concluded that both synthetic procedures yield very similar Ni nanoparticles, and thus evidenced that the new methodology developed in this work allows rapid access to NHC-stabilized nanoparticles without the need for a basic pre-treatment. With these results in hand, supported Ni nanocatalysts were synthesized following the same methodology in the presence of multiwalled carbon nanotubes (MWCNTs). The amount of the NHC-based ligand used during the synthesis was varied from 0.2 to 0.5 to 1 equivalent per Ni. TEM analysis of the resulting hybrid material is shown in Fig. 2. Interestingly, the TEM micrographs of **Ni-0.2@CNTs** and **Ni-0.5@CNTs** revealed the formation of very similar nanoparticles with no significant differences in size, shape and distribution since both exhibited a diameter of *ca.* 3.6 ± 0.8 nm.

It is remarkable that an increase of the mean particle size and size distribution was observed in comparison with the

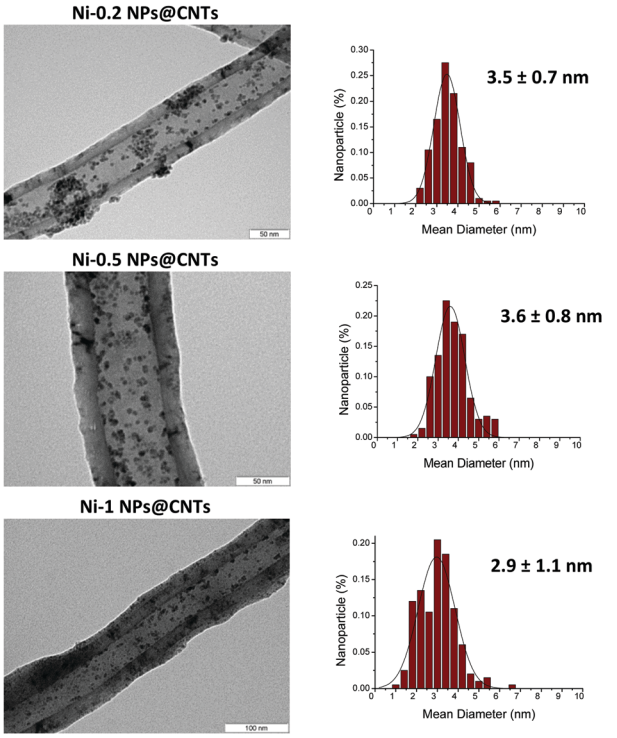

Fig. 2 TEM micrographs and size distributions of supported **Ni-0.2**, **Ni-0.5** and **Ni-1 NPs@CNTs**.

colloidal system. When the amount of the NHC-based stabilizer was increased to 1 equivalent per Ni (**Ni-1@CNTs**), a wider distribution was observed with no significant difference in size with respect to the colloidal system. In general, the small Ni nanoparticles were mostly deposited in the inner cavity of the CNTs, as confirmed by STEM (Fig. 3). The supported nanoparticles were characterized by XRD analysis, evidencing the presence of Ni crystalline systems with fcc packing (Fig. S11, ESI†). XPS measurements (Fig. S12, ESI†) again revealed a high surface NiO content (82.9 at%) due to the strong oxygen sensitivity of the nanoparticles even after immobilization onto CNTs. However, after Ar sputtering the metal content increased (72.7 at%). Finally, TGA and ICP revealed a nickel content in **Ni-Me$_2$Im@CNTs** that was similar to the nominal loading (10 wt%) with values of 10.0 wt% and 8.8 wt%, respectively.

Next, the catalytic performance of the NPs was evaluated in the semi-hydrogenation of internal alkynes. The results are summarized in Table 1. First, the catalytic performances of **Ni-0.2@CNTs**, **Ni-0.5@CNTs** and **Ni-1@CNTs** were compared

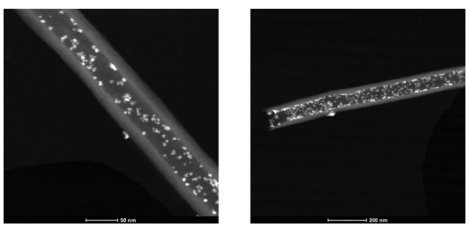

Fig. 3 STEM micrographs of **Ni-0.5@CNTs**.

Table 1 Catalytic semi-hydrogenation of internal alkynes using **NiMe$_2$ImNPs@CNTs**[a]

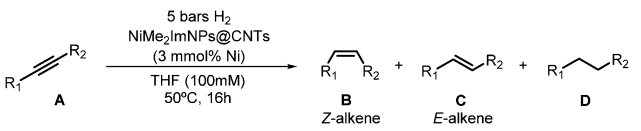

Entry	NiNPs@CNTs	R_1	R_2	Conv.[b] (yield B)[c]	B/C[b]	% D[b]
1	**Ni-0.2@CNTs**	Ph	Ph	100	94/6	0
2	**Ni-0.5@CNTs**	Ph	Ph	100 (97)	97/3	0
3	**Ni-1@CNTs**	Ph	Ph	78	78/22	0
4	**Ni-0.5@CNTs**	$(CH_2)_2CH_3$	$(CH_2)_2CH_3$	100 (91)	99/1	0
5	**Ni-0.5@CNTs**	CH_3	$(CH_2)_4CH_3$	81 (90)	98/2	10
6	**Ni-0.5@CNTs**	CH_2CH_3	Ph	100 (70)	94/6	12
7	**Ni-0.5@CNTs**	CH_2OH	Ph	100 (80)	96/4	13

[a] General conditions: 1 mmol of the substrate, 3 mol% of Ni, 10 ml of THF, 50 °C, 5 bar H_2, t = 16 h. [b] Determined by GC-MS spectrometry and NMR analysis. [c] Isolated yield.

using diphenylacetylene as a model substrate using 3 mol% of Ni at 50 °C and under 5 bar of H_2. After 16 h, full conversion was achieved for **Ni-0.2@CNTs** and **Ni-0.5@CNTs**, while a lower value was measured for **Ni-1@CNTs** (Table 1, entries 1–3). This indicated that the large amount of NHC used during the synthesis of the latter nanocatalyst could hinder the substrate coordination at their surface. In all cases, no over-hydrogenation product was detected while a distinct degree of stereoselectivity was measured: using **Ni-0.2@CNTs**, excellent selectivity (94%) to the *Z*-alkene was observed, while using **Ni-0.5@CNTs** as a catalytic system, diphenylacetylene was selectively converted to (*Z*)-stilbene in quantitative yield (Table 1, entry 2). In contrast, using **Ni-1@CNTs**, a drop in selectivity was detected.

In view of these results, the reaction using **Ni-0.5@CNTs** as a catalytic system was repeated and monitored over time (Fig. 4). The total conversion of the substrate was observed after a reaction time of 7 hours with total selectivity for the corresponding (*Z*)-alkene. Interestingly, no over-hydrogenation of the substrate into the corresponding alkane was observed even after 24 hours of reaction.

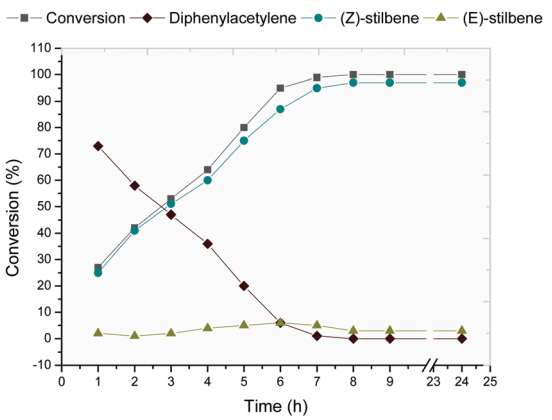

Fig. 4 Evolution in time of diphenylacetylene semi-hydrogenation in the presence of **Ni-0.5@CNTs** at 50 °C, 5 bar H_2 for 24 h.

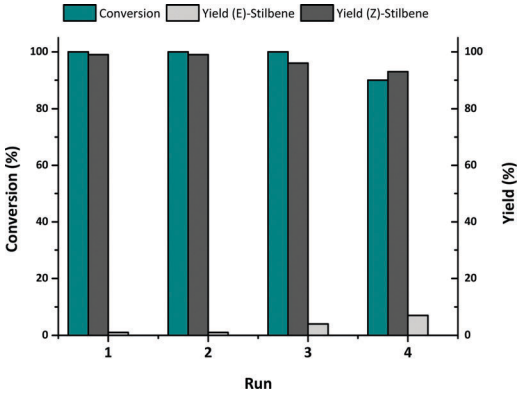

Fig. 5 Recycling experiment of the hydrogenation of diphenylacetylene over **Ni-0.5@CNTs** at 50 °C, 5 bar H_2 for 7 h.

The remaining solution after the catalytic reaction was analysed by inductively coupled plasma (ICP), revealing a nickel content of 0.008% with respect to all Ni initially introduced. Furthermore, no evolution of the reaction was observed when the semi-hydrogenation of diphenylacetylene was tested using the remaining solution of a catalytic test after filtration of the heterogeneous catalyst. These results indicated that no relevant leaching had taken place under the reaction conditions.

Next, we examined the application of the optimized catalyst system for a broader scope of internal alkynes (Table 1, entries 4–7). When 4-octyne was tested as a substrate (entry 4), the corresponding (*Z*)-alkene was again obtained in quantitative yield. However, when 2-octyne was used (entry 5), 81% conversion was measured and a mixture of alkene and alkane was observed. However, the *Z*/*E* ratio remained at *ca.* 98%. In the case of a 1-phenyl-1-butyne substrate, a greater amount of alkane was obtained (12%) at 100% conversion and the selectivity *Z*/*E* was slightly lower (*ca.* 92%) (entry 6). In the hydrogenation of 3-phenyl-2-propyn-1-ol (entry 7), the selective formation of the (*Z*)-alkene was observed, but 13% of the over-hydrogenated product was detected with full conversion.

To evaluate the robustness of these catalysts, **$NiMe_2$Im-0.5 NPs@CNTs** were recycled several times in the hydrogenation of diphenylacetylene as a model substrate (Fig. 5). Neither relevant loss of activity nor selectivity was observed over 3 runs although a slight decrease in activity was observed in the last run.

In conclusion, a new procedure for synthesizing small and well-defined NHC-stabilized NiNPs based on the decarboxylation of the corresponding imidazolium carboxylate zwitterionic salt has been developed. This methodology was employed for the synthesis of colloidal NiNPs and for the immobilization of NiNPs onto carbon nanotubes by a simple ''one-pot'' procedure without surface modification. These NPs were thoroughly characterised and the supported NPs revealed efficient catalysts in the selective hydrogenation of terminal alkynes into the corresponding (*Z*)-alkenes under very mild reaction conditions. Furthermore, these heterogeneous catalysts can be readily recovered by simple filtration and reused 3 times without relevant decrease in activity.

The authors are grateful to the European Union's Horizon 2020 research and innovation programme (ref. 677471), the TERRA project and the Ministerio de Economia y Competitividad and the Fondo Europeo de Desarrollo Regional FEDER (CTQ2016-75016-R, AEI/FEDER, UE) for funding.

Notes and references

1 G. Schmid, *Nanoparticles*, From theory to applications, Weinheim, 2004.
2 A. Roucoux, J. Schulz and H. Patin, *Chem. Rev.*, 2002, **102**, 3757–3778.
3 M. N. Hopkinson, C. Richter, M. Schedler and F. Glorius, *Nature*, 2014, **510**, 485–496.
4 D. Canseco-Gonzalez, A. Petronilho, H. Mueller-Bunz, K. Ohmatsu, T. Ooi and M. Albrecht, *J. Am. Chem. Soc.*, 2013, **135**, 13193–13203.
5 E. C. Hurst, K. Wilson, I. J. S. Fairlamb and V. Chechik, *New J. Chem.*, 2009, **33**, 1837–1840.
6 J. Vignolle and T. D. Tilley, *Chem. Commun.*, 2009, 7230–7232.
7 A. V. Zhukhovitskiy, M. G. Mavros, T. Van Voorhis and J. A. Johnson, *J. Am. Chem. Soc.*, 2013, **135**, 7418–7421.
8 G. Wang, A. Ruhling, S. Amirjalayer, M. Knor, J. B. Ernst, C. Richter, H.-J. Gao, A. Timmer, H.-Y. Gao, N. L. Doltsinis, F. Glorius and H. Fuchs, *Nat. Chem.*, 2017, **9**, 152–156.
9 K. V. S. Ranganath, J. Kloesges, A. H. Schaefer and F. Glorius, *Angew. Chem., Int. Ed.*, 2010, **49**, 7786–7789.
10 L. S. Ott, M. L. Cline, M. Deetlefs, K. R. Seddon and R. G. Finke, *J. Am. Chem. Soc.*, 2005, **127**, 5758–5759.
11 P. Lara, O. Rivada-Wheelaghan, S. Conejero, R. Poteau, K. Philippot and B. Chaudret, *Angew. Chem., Int. Ed.*, 2011, **50**, 12080–12084.
12 L. M. Martinez-Prieto, A. Ferry, P. Lara, C. Richter, K. Philippot, F. Glorius and B. Chaudret, *Chem. – Eur. J.*, 2015, **21**, 17495–17502.
13 J.-F. Soule, H. Miyamura and S. Kobayashi, *J. Am. Chem. Soc.*, 2013, **135**, 10602–10605.
14 C. Richter, K. Schaepe, F. Glorius and B. J. Ravoo, *Chem. Commun.*, 2014, **50**, 3204–3207.
15 A. M. Voutchkova, L. N. Appelhans, A. R. Chianese and R. H. Crabtree, *J. Am. Chem. Soc.*, 2005, **127**, 17624–17625.
16 J. D. Holbrey, W. M. Reichert, I. Tkatchenko, E. Bouajila, O. Walter, I. Tommasi and R. D. Rogers, *Chem. Commun.*, 2003, 28–29.
17 D. M. Denning and D. E. Falvey, *J. Org. Chem.*, 2014, **79**, 4293–4299.
18 J. G. de Vries and C. J. Elsevier, *The Handbook of Homogeneous Hydrogenation*, Wiley-VCH, 2008.
19 M. Crespo-Quesada, F. Cardenas-Lizana, A.-L. Dessimoz and L. Kiwi-Minsker, *ACS Catal.*, 2012, **2**, 1773–1786.
20 H. Konnerth and M. H. G. Prechtl, *Chem. Commun.*, 2016, **52**, 9129–9132.
21 A. Molnar, A. Sarkany and M. Varga, *J. Mol. Catal. A: Chem.*, 2001, **173**, 185–221.
22 E. Bayer and W. Schumann, *J. Chem. Soc., Chem. Commun.*, 1986, 949–952.
23 E. J. Garcia-Suarez, A. M. Balu, M. Tristany, A. B. Garcia, K. Philippot and R. Luque, *Green Chem.*, 2012, **14**, 1434–1439.
24 P. Lara, L. M. Martinez-Prieto, M. Rosello-Merino, C. Richter, F. Glorius, S. Conejero, K. Philippot and B. Chaudret, *Nano-Struct. Nano-Objects*, 2016, **6**, 39–45.
25 E. A. Baquero, S. Tricard, J. C. Flores, E. de Jesus and B. Chaudret, *Angew. Chem., Int. Ed.*, 2014, **53**, 13220–13224.